



AENSI Journals

Australian Journal of Basic and Applied Sciences

ISSN:1991-8178

Journal home page: www.ajbasweb.com



A Comparative Study of Radiation Dose versus Image Quality between Different Low-Dose Mdct Protocols in Maxillary Sinus Examination

¹Abeer Abdulkareem Al-Mashraqi, ²Eman Abd Elaziz Ahmed, ³Nashwa Salah Mohamed, ⁴Nader Abd Elsalam Elsherbini, ⁵Omar Osman Moawia.

¹Lecturer, Department of Oral Radiology, Faculty of Dentistry, Ibb University, Ibb, Republic of Yemen.

²Professor, Department of Oral and Maxillofacial Radiology, Faculty of Oral and Dental Medicine, Cairo University, Cairo, Egypt; Professor and Head of Oral and Maxillofacial Radiology Department, Faculty of Oral and Dental Surgery, Misr university for science and technology, Giza, Egypt.

³Professor, Department of Oral and Maxillofacial Radiology, Faculty of Oral and Dental Medicine, Cairo University, Cairo, Egypt; Professor of Oral and Maxillofacial Radiology Department, Faculty of Oral and Dental Medicine, Misr International University, Cairo, Egypt.

⁴Professor of Medical Radiation Physics, Kasr Al-Aini Center of oncology and Nuclear Medicine, Faculty of Medicine, Cairo University, Cairo, Egypt.

⁵Professors of Radiology Department, Kasr Al-Aini, Faculty of Medicine, Cairo University, Cairo, Egypt.

ARTICLE INFO

Article history:

Received 25 January 2014

Received in revised form

8 April 2014

Accepted 20 April 2014

Available online 10 May 2014

Keywords:

Radiation dose, Image quality, Low-dose MDCT

ABSTRACT

Background: With the increased use of computed tomography scanners for maxillary sinus examinations, the radiation exposure is increased especially to the eye lens, salivary glands, and the thyroid glands. Previous studies conducted on the sinus examination were focused mainly on the eye lens only. **Objective:** This study aimed to compare the doses to the eye lens, thyroid gland, and salivary glands versus image quality obtained by the standard and the low-dose multi-detector computed tomography during maxillary sinus examination. **Results:** Statistically significant differences were found between all low-dose MDCT protocols and the standard MDCT protocol in radiation dose with P-value (<0.001). The measured organ doses received by the eyes were ranged from 3mGy to 31.4mGy, the thyroid gland from 0.53mGy to 2.9mGy, and salivary glands from 2.96mGy to 24.9mGy. The subjective and objective image quality revealed unacceptable image quality for protocol X (20 effective mAs), while protocols VIII (32 effective mAs) and IX (25 effective mAs) revealed diagnostic images quality. **Conclusion:** Low-dose multi-detector computed tomography for the sinus examination can yield a diagnostic image quality with doses for the most sensitive organs of the head and neck eight times lower than that of the standard multi-detector computed tomography.

© 2014 AENSI Publisher All rights reserved.

To Cite This Article: Abeer Abdulkareem Al-Mashraqi, Eman Abd Elaziz Ahmed, Nashwa Salah Mohamed, Nader Abd Elsalam Elsherbini, Omar Osman Moawia., A Comparative Study of Radiation Dose versus Image Quality between Different Low-Dose Mdct Protocols in Maxillary Sinus Examination. *Aust. J. Basic & Appl. Sci.*, 8(6): 362-370, 2014

INTRODUCTION

The maxillary sinus is the largest and the most important member of a group of structures collectively known as paranasal sinuses. It is a frequent site for pathologies of odontogenic and non-odontogenic origins (Perrella, Rocha and Cavalcanti, 2003; Sales and Cavalcanti, 2009). Maxillary sinus involvement must be carefully assessed because orbital damage and spreading of associated infections or any pathology could lead to local and systemic compromise to the patient. So, suspicion of maxillary sinus involvement means that radiographic evaluation is mandatory (Tan *et al.*, 2008; Sales and Cavalcanti, 2009).

Computed tomography (CT) is the gold standard for sinus examination. It has almost replaced plain film examinations in the work-up for sinus diseases, especially for ruling out any suspicion of associated orbital involvement and revealing the spread and intracranial extension of infectious process. Additionally, it is widely performed in the imaging work-up of sinus pathologies and for surgical planning (Anzai *et al.*, 2004; Ling and Kountakis, 2006; Kim *et al.*, 2007).

However, the known disadvantage of CT imaging is the high radiation dose that affects the radiosensitive organs within the scanning field (the thyroid gland, the eye lens, and salivary glands). Even with new generations of multidetector CT (MDCT), this dose still making alarm by its possible side effects on these radiosensitive organs (Zammit-Maempel *et al.*, 2003; Loubele *et al.*, 2009). Recently, there is a new low-dose

Corresponding Author: Abeer Abdulkareem Al-Mashraqi, Lecturer, Department of Oral Radiology, Faculty of Dentistry, Ibb University, Ibb, Republic of Yemen.
E-mail: abeerradiology@gmail.com

CT protocol that offers considerable dose reduction which reduces the dose to approximately 77% without loss of diagnostic image quality (Bianchi *et al.*, 2005; Mulkens *et al.*, 2005; Lam *et al.*, 2009; Stelmachet *et al.*, 2010). This dose reduction depends on several factors, including the type of scanner, tube current, and voltage used.

Most of previous sinus studies were focused on radiation dose to the eye lens only. Other studies conducted on salivary gland were focused on standard MDCT protocol without concern to low-dose MDCT protocols. However, only one study was concerned with the measured dose of the thyroid gland in both standard and low-dose MDCT protocols (Zammit-Maempel *et al.*, 2003). Moreover, most of these studies didn't take into consideration the image quality of different MDCT protocols. Accordingly, the aim of the present study was to compare the doses of the eye lens, thyroid gland, and salivary glands and image quality of the standard and low-dose MDCT protocols in maxillary sinus examination.

MATERIAL AND METHODS

A head phantom and TLDs:

An anthropomorphic head and neck Alderson RANDO (The RANDO® Phantom, Alderson Research Laboratories Inc., Stanford, CT, USA) was used. It consists of a human skull embedded in an isocyanic rubber equivalent to human soft tissues, in which the radiation absorption and spread match that of human tissue. This phantom consists of ten transverse sections with 2.5cm thickness. Each section is perforated to accommodate thermoluminescent dosimeter chips (TLD-700). Thermoluminescent dosimeter system (RADOS) is composed of chips, slide, and holder. The TLD chips based on lithium fluoride, whose dimensions are 4 mm diameter and 1 mm thickness, were used to record radiation dose at selected locations in the head and neck region of the RANDO phantom.

Imaging system and scanning parameters:

Multi-detector computed tomography (Activion 16, Toshiba-Medical system, Japan) was used with ten protocols of different scanning parameters. These protocols were chosen by changing in mAs and pitch factor (PF) starting from the standard CT protocol (according to manufacturer) until the cutoff value of a non-diagnostic image quality was reached (Table 1). This scanning was performed with a tilted gantry that was parallel to the Frankfort plane. Firstly, the scout image was performed to locate the scan area with 30mA and 120kvp. Then, the area of interest was scanned. The image matrix consisted of 512×512 pixels. High resolution was chosen for the data acquisition and for the image reconstruction. After that, the axial images were reconstructed to produce sagittal, coronal, and 3D image.

Table (1): parameters of the ten MDCT protocols:

| Protocol NO. | KV | RT | mA | mAs | PF | EmAs | collimation | ST |
|--------------|-----|------|-----|------|------|------|-------------|----|
| I | 120 | 0.75 | 130 | 97 | 0.69 | 142 | 1x16 | 1 |
| II | 120 | 0.75 | 130 | 97 | 0.93 | 104 | 1x16 | 1 |
| III | 120 | 0.75 | 70 | 52 | 0.69 | 77 | 1x16 | 1 |
| IV | 120 | 0.75 | 130 | 97 | 1.5 | 65 | 1x16 | 1 |
| V | 120 | 0.75 | 70 | 52 | 0.93 | 56 | 1x16 | 1 |
| VI | 120 | 0.75 | 50 | 37.5 | 0.93 | 40 | 1x16 | 1 |
| VII | 120 | 0.75 | 70 | 52 | 1.5 | 35 | 1x16 | 1 |
| VIII | 120 | 0.75 | 40 | 30 | 0.93 | 32 | 1x16 | 1 |
| IX | 120 | 0.75 | 50 | 37.5 | 1.5 | 25 | 1x16 | 1 |
| X | 120 | 0.75 | 40 | 30 | 1.5 | 20 | 1x16 | 1 |

RT: rotation time, PF: pitch factor, EmAs: effective mAs, ST: slice thickness in mm.

Radiation dose measurement:

TLD system, TLD reader, TLD irradiator, and RANDO phantom were used to measure the dose as follows:

I- Placement of TLDs on RANDO phantom and scanning of the phantom:

Five sensitive organs were chosen on the RANDO phantom for placement of TLDs (eye (inner and outer canthus), three salivary glands, and thyroid gland). These organs and the number of each slice of the phantom were listed in (Fig.1). A total of 18 TLDs were used for each scan that was distributed as three chips in each sensitive organ. After that, the slices of the phantom were assembled and screwed well. Then, the TLDs that used to measure the dose to the eyes were wrapped with paper and fixed on the inner and outer canthus on the phantom by a plaster. Scanning of the phantom with all protocols one by one was performed and the same steps were repeated twice for each protocol to provide a reliable measure of radiation in the dosimeters.

II- Reading of the TLDs:

The readout of the TLDs dose values was obtained with a TLDs reader system (Alnor Dosacus TLD-reader) and within a range of 24 hours from exposure. The TLDs were installed in the Alnor slide and each slide number was used as a code for each sensitive organ. Then, the TLDs slides were loaded in Alnor cartridge and

then read on the TLDs reader. The organ dose results were the average value of the evaluated data of the three TLDs per measuring point.

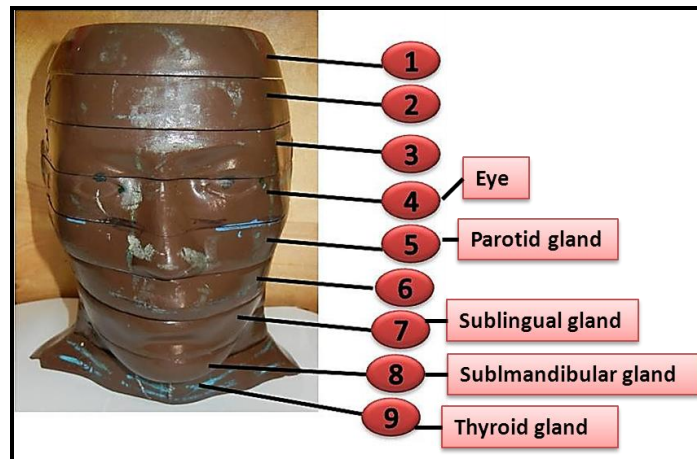


Fig. 1: The level of the sensitive organs on the RANDO phantom.

III- Measurement of TLD sensitivity factor:

The chips sensitivity was firstly determined by irradiating the chips to a known radiation dose and the corresponding charges were recorded. Then, the sensitivity was determined by dividing the recorded charge by the dose of each chip. RADOS irradiator was used for this purpose.

Image quality:

Objective assessment:

A cylindrical water-filled Perspex phantom was scanned to measure the image noise of all MDCT protocols. A measurement of image noise (a measurement of the fluctuations of CT number) was performed using regions of interest (ROIs) on a scan of a uniform phantom without application of filter algorithms. A statistical ROI function (available on most CT scanners) allows users to place a rectangular or oval ROI on the image (150 cm² was fixed for all protocols), within which is calculated the average and standard deviation (SD) of the CT numbers for the enclosed pixels. The SD indicates the magnitude of random fluctuations in the CT number that is related to noise: The larger the SD, the higher the image noise (**Goldman, 2007**) (**Fig. 2**).

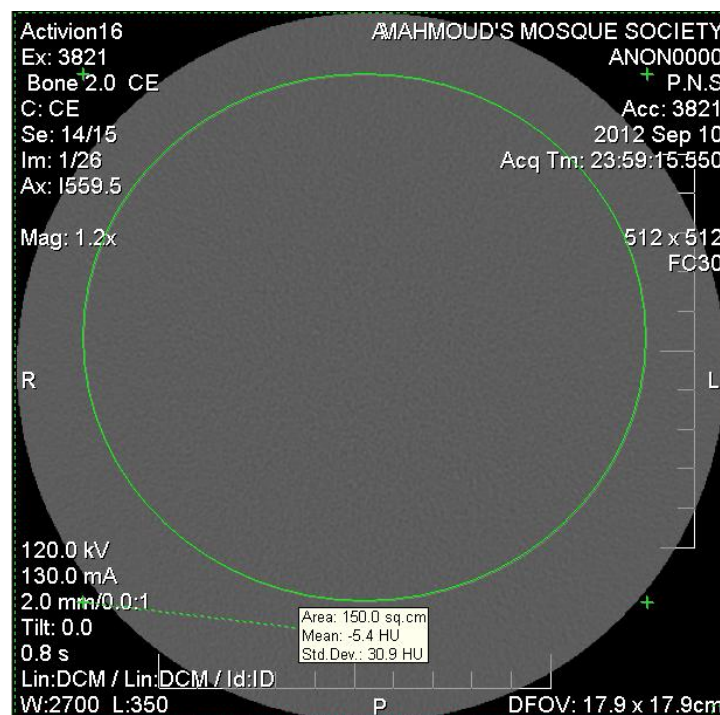


Fig. 2: The measurement of image noise.

Subjective assessment:

After the scanning of the phantom, the volume data sets of the RANDO phantom of different MDCT protocols were stored in a DICOM format and projected on a 3D workstation to evaluate image quality. These images were assessed blindly by two experienced oral and maxillofacial radiologists and one experienced general radiologist. The evaluation was performed for the overall image quality that had little image noise and scored from 1 to 4 as; 1 = very good, 2 = good, 3 = acceptable, 4 = unacceptable. The image quality was assessed for both bone and soft tissue windows to preserve the diagnostic image quality for both hard and soft tissues (**Fig. 3, 4, and 5**).

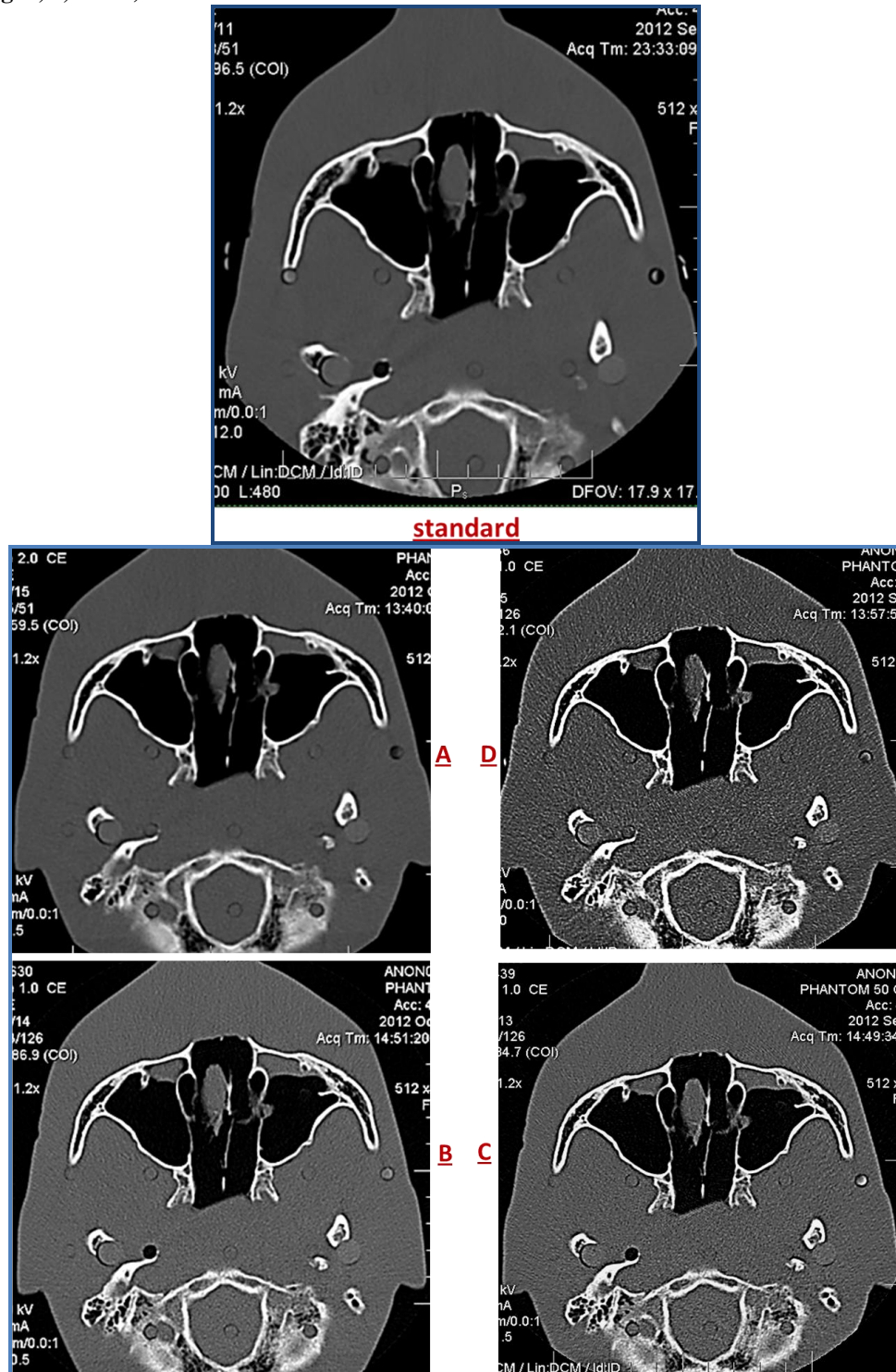


Fig. 3: Axial sections of bone window scanned at levels of maxillary sinus revealed the variations in image quality (image noise) of different MDCT protocols; (Standard) Standard MDCT protocol, (A) Protocol VII, (B) Protocol VIII, (C) Protocol IX, and (D) Protocol X.

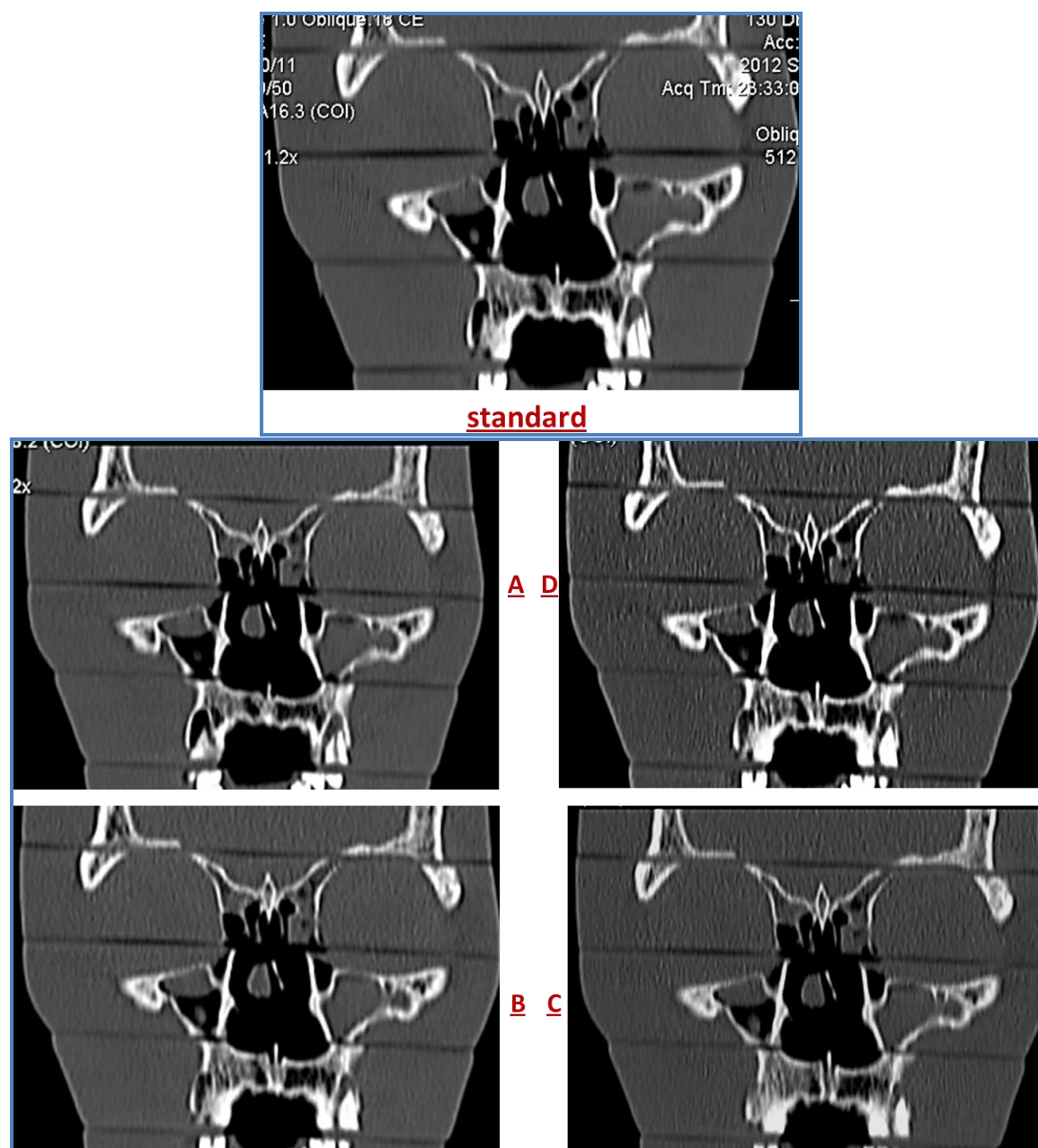


Fig. 4: Coronal sections of bone window scanned at levels of maxillary sinus revealed the variations in image quality (image noise) of different MDCT protocols; (Standard) Standard MDCT protocol, (A) Protocol VII, (B) Protocol VIII, (C) Protocol IX, and (D) Protocol X.

Statistical analysis:

Numerical data were presented as mean and SD values. Data were explored for normality using Kolmogorov-Smirnov and Shapiro-Wilk tests. Doses values and objective image noise values revealed parametric distribution. Repeated measures ANOVA test followed by Bonferroni's post hoc test for pair-wise comparisons were used to compare between the different protocols. However, the scoring data of image quality assessment is non-parametric data. Friedman test was used to compare between the different protocols. The significance level was set at $P \leq 0.05$. Statistical analysis was performed with IBM® SPSS® Statistics Version 20 for Windows.

Results:

I- Organ dose:

The measured organ doses at the level of the TLD locations of the eyes, salivary glands, and thyroid gland in the RANDO phantom were presented in Table 2 for five protocols only. In the eyes: protocol I revealed the highest mean doses with a statistically significant difference with other protocols. Protocols VII, VIII, IX, and X

revealed lower mean doses than protocol I without a statistically significant difference between each other. Additionally, in the thyroid gland and *salivary glands*: protocol I followed by protocol VII revealed the highest mean doses with a statistically significant difference with each other and with other protocols. Protocols VIII, IX, and X revealed lower mean doses than protocols I and VII with a statistically insignificant difference between each other.

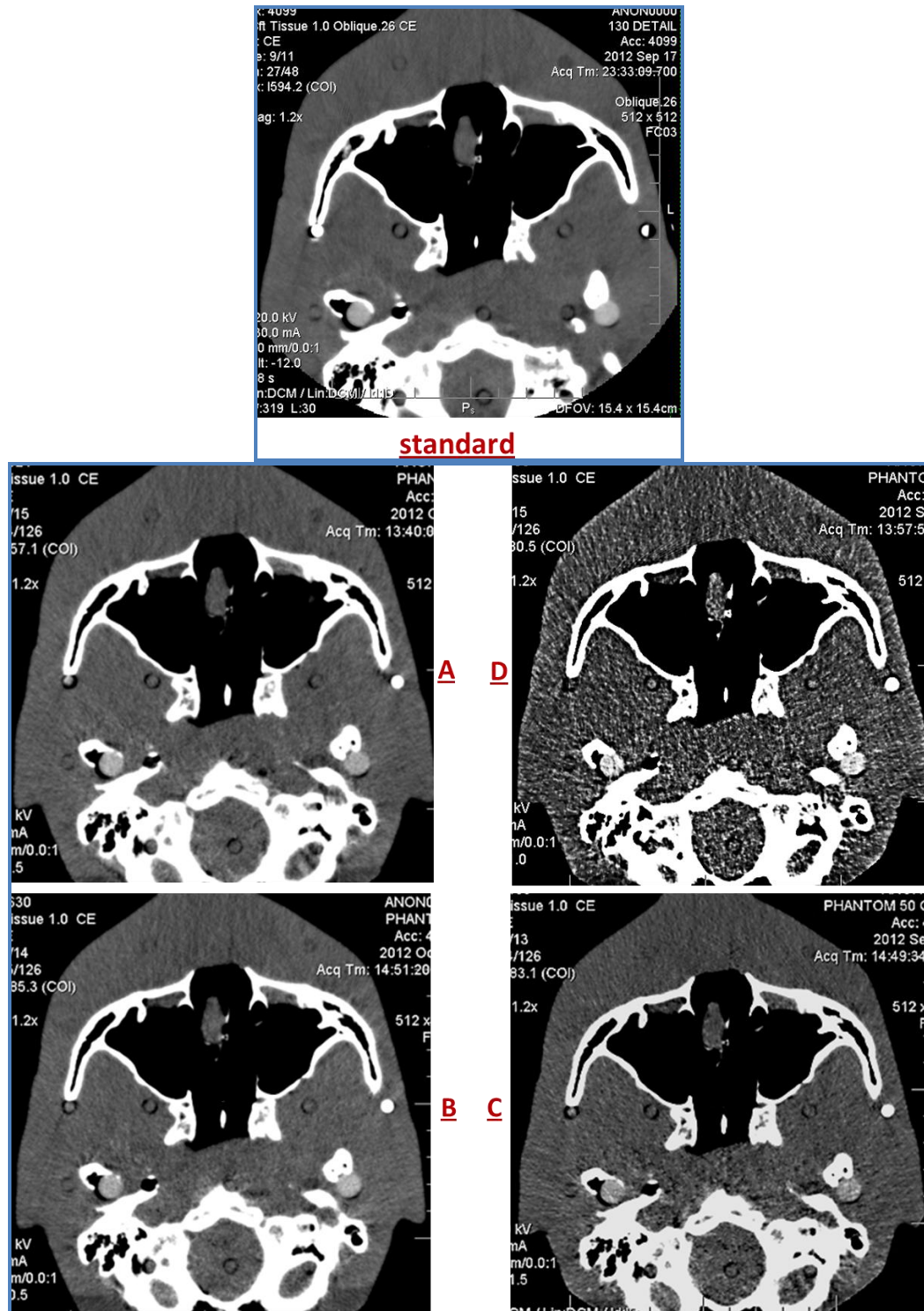


Fig. 5: Axial sections of soft tissue window scanned at levels of maxillary sinus revealed the variations in image quality (image noise) of different MDCT protocols; (Standard) Standard MDCT protocol, (A) Protocol VII, (B) Protocol VIII, (C) Protocol IX, and (D) Protocol X.

Table (2): Mean, standard deviation (SD), and P-value for the comparison between doses (mGy) of a standard MDCT protocol and low-dose MDCT protocols in different organs:

| Organs | Protocol I | | Protocol VII | | Protocol VIII | | Protocol IX | | Protocol X | | P-value |
|------------|-------------------|------|------------------|------|-------------------|------|-------------------|------|-------------------|------|---------|
| | Mean | SD | Mean | SD | Mean | SD | Mean | SD | Mean | SD | |
| Eye | 31.4 ^a | 1.5 | 6.4 ^b | 0.27 | 4.2 ^b | 0.04 | 3.7 ^b | 0.12 | 3 ^b | 0.10 | <0.001* |
| Thyroid G | 2.9 ^a | 0.12 | 0.9 ^b | 0.01 | 0.62 ^c | 0.01 | 0.58 ^c | 0.01 | 0.53 ^c | 0.01 | <0.001* |
| Salivary G | 24.9 ^a | 0.45 | 5.1 ^b | 0.13 | 3.98 ^c | 0.11 | 3.5 ^c | 0.14 | 2.95 ^c | 0.05 | <0.001* |

*: Significant at $P \leq 0.05$, Different letters in the same row are statistically significantly different according to Bonferroni's test.

II- Image quality:

Objective assessment of all protocols presented in Table 3. Protocol I showed the lowest mean score of image noise with a statistically significant difference with other protocols. Protocol X showed the statistically significant highest mean score of image noise with a statistically significant difference with other protocols. Statistically insignificant difference between protocols VII, VIII, and IX were found.

Subjective assessment of all protocols was presented in Table 3. Protocol I revealed the statistically significant lowest mean score of image noise without a statistically significant difference with other protocols except protocol X. Protocol X showed the statistically significant highest mean score of image noise.

Table (3): Mean, standard deviation (SD), and P-value for the comparison between objective and subjective assessments of image quality of a standard MDCT protocol and low-dose MDCT protocols:

| Assessment | Protocol I | | Protocol VII | | Protocol VIII | | Protocol IX | | Protocol X | | P-value |
|------------|-------------------|-----|-------------------|-----|-------------------|------|-------------------|-----|-------------------|-----|---------|
| | Mean | SD | Mean | SD | Mean | SD | Mean | SD | Mean | SD | |
| Objective | 30.8 ^a | 5.6 | 56.3 ^b | 7.2 | 63.4 ^b | 4.1 | 71.6 ^b | 6.2 | 84.6 ^c | 9.3 | <0.001* |
| subjective | 1 ^a | 0 | 2 ^a | 0 | 2.33 ^a | 0.58 | 3 ^a | 0 | 4 ^b | 0 | <0.02* |

*: Significant at $P \leq 0.05$, Different letters in the same row are statistically significantly different.

Discussion:

The radiation exposure to the population was increased due to the increased availability of CT scanners and the increased number of CT examinations. In the early nineties, CT constituted about 2% to 3% of all radiologic examinations and contributed to about 20% to 30% of the total radiation load from medical use of ionizing radiation (Shrimpton *et al.*, 1991). A later report revealed that CT accounts up to 11% of all radiology procedures in the United States and constitutes approximately two thirds of the collective medical radiation dose (Mettler *et al.*, 2000). Especially, the eye lenses, salivary glands, and the thyroid glands are vulnerable sensitive organs, which are usually subjected to high radiation doses from CT of head and neck (Czechowski *et al.*, 2001). The advent of new generation CT scanners with improved spatial and contrast resolutions allow maintaining scan quality at a much lower radiation dose and thus, revolutionized diagnostic imaging. If these facts are taken into consideration, the optimization of the radiation doses will be an important issue in the diagnostic radiology.

This research was conducted on maxillary sinus because it is one of the highly contrasted structures, since the diagnostic quality of images of these structures is not substantially affected by dose reduction (Homolka *et al.*, 2001). Computed tomography has become the method of choice for confirming and determining the maxillary sinus diseases and their extension (Czechowski *et al.*, 2001; Zammit-Maempel *et al.*, 2003). Therefore, standard CT protocol was considered a gold standard in this study.

The mAs and pitch factor were changed in the present research even been reached the lowest possible radiation dose with acceptable diagnostic image quality. This was conducted by reduced mAs and increased PF, which is in consistent with other studies (Tack *et al.*, 2003; Mulken *et al.*, 2005). The mAs was changed because it is one of the most important factor affecting dose and most studies depended on it to reduce dose. It acts by decreased the photons numbers emerging from the device resulting in radiation dose reduction. Additionally, PE is another important factor that limited only to MDCT scanner and depends on increased table speed to decreased radiation dose. However, the PF was not increased more than 1.5 to avoid the effect on image reconstruction that documented in other study (Goldman, 2007). Additionally, gantry tilting was performed with an angle parallel to the Frankfort plane because it causes a significant dose reduction especially on the eyes.

Ten MDCT protocols were selected to study with them until the cutoff value was reached at 20 effective mAs. This cutoff value is in consistent with the study of Hojreh *et al.* (2005). From ten protocols, only two protocols matched the lowest radiation dose with a good and an acceptable diagnostic image quality. As a result of that, the results of only five protocols were presented. These protocols were a standard protocol (protocol I), two matched protocols (protocols VIII and IX), one protocol lower than the two matched protocols (protocols X), and one protocol higher than the two matched protocols (protocol VII).

The dose received by the eye in the standard protocol was 31.4mGy, which appeared to be within the range of previously measured values with spiral scans in other studies (Cohnen *et al.*, 1998; Dammann *et al.*, 2000; Zammit-Maempel *et al.*, 2003; Bassim *et al.*, 2005). Lower doses, in the range of 10-20 mGy, had been reported in other studies (MacLennan *et al.*, 1995; Bernhardt *et al.*, 1998; Sohaib *et al.*, 2001, Tan *et al.*, 2008). However, these had been typically obtained with different protocols. The dose of the eye in the low-dose MDCT protocols

ranged from 3 to 6.3mGy, which is in consistent with the finding of other low-dose CT studies (Kearney *et al.*, 1997; Sohaib *et al.*, 2001; Zammit-Maempel *et al.*, 2003; Lam *et al.*, 2009). These measured doses are still much lower than the 500 mGy threshold for lens cataract and thus appear to be clinically safe.

The dose to the thyroid gland from different MDCT protocols reported a comparable measured value with the study conducted by Zammit-Maempel *et al.* (2003) who worked in both the standard and low-dose MDCT protocols in the patients of paranasal sinuses with a 4-MDCT scanner. A lower dose was reported in the study of Zammit-Maempel *et al.* (1996) who achieved these measured values from coronal cuts and from different parameters. The relative risk of dose-dependent thyroid cancer was reported in the literature of radiotherapy as 3-6 Gy dose during childhood (Cardis *et al.*, 2005; Abend *et al.*, 2012). This value is so far from the dose of the diagnostic imaging.

In relation to the radiation effect on the salivary glands from diagnostic imaging; no studies in the literature were found. Most literature on radiation therapy for head and neck cancer clearly reveals a dose-dependent atrophy and dysfunction. Stephens *et al.* (1986 and 1991) reported tissue injury with doses as low as 2500 mGy in rhesus monkeys, which remains well above the measured dose in this study and is unlikely to be of a clinical significance. The dose received by the parotid gland in the current study from the standard protocol revealed a comparable value to that recorded by Bassim *et al.* (2005) who used the same protocol parameters.

The objective assessment of image noise in this study is in consistent with the study accomplished by Hojreh *et al.* (2005) who found a comparable image noise for each MDCT protocol used in this study. Additionally, the subjective assessment of image quality in this research is in agreement with other studies performed by Abul-Kasim *et al.* (2011) and Jeong *et al.* (2012) who reported a good image quality of RANDO phantom in all MDCT protocols.

The subjective assessment was performed to the overall image noise in the head phantom rather than the evaluation of different anatomical landmarks. This evaluation couldn't be applied due to the destruction of some detailed anatomical landmarks in the head phantom. Thus, objective assessment was used with the subjective assessment to confirm the result of each other. The purpose of the image quality assessment in this research was to determine the cutoff value that get low radiation dose but with a non-diagnostic image quality. There was no difference between both assessments in the determination of the cutoff value. Both assessments were revealed a non-diagnostic image quality of protocol X with a statistically significant difference with the standard MDCT protocol.

A statistically significant reduction in doses of the three sensitive organs measured in this study ranged from 80% to 87% was obtained. This is in consistent with other studies accomplished by cohnen *et al.* (2000), czechwski *et al.* (2000), Lam *et al.* (2009), Stelmachet *et al.* (2010), and Yu *et al.* (2010) who concluded that the dose of CT could be reduced seven to eight times with maintenance of the diagnostic image quality. Despite the evidence of the dose reduction causes increase in the image noise that automatically affects the image quality, the two matched protocols (protocols VIII and IX) obtained in this study had a low radiation dose and preserved the diagnostic image quality.

Conclusions:

Low-dose MDCT for the sinuses can yield a diagnostic image quality with doses for the most sensitive organs of the head and neck eight times lower than that of the standard MDCT protocol.

Further studies on patients with maxillary sinus diseases using the recommended protocols in this study are requested.

REFERENCES

Abend, M., R.M. Pfeiffer, C. Ruf, M. Hatch, T.I. Bogdanova, M.D. Tronko, A. Riecke and J. Hartmann, 2012. Iodine-131 dose dependent gene expression in thyroid cancers and corresponding normal tissues following the Chernobyl accident. *PLoS One*, 7(7): e39103.

Anzai, Y., E.A. Weymuller, B. Yueh, N. Maronian and J.G. Jarvik, 2004. The Impact of Sinus Computed Tomography on Treatment Decisions for Chronic Sinusitis. *Arch Otolaryngol Head Neck Surg.*, 130(4): 423-428.

Bassim, M.K., C.S. Ebert, R.C. Sit and B.A. Senior, 2005. Radiation dose to the eyes and parotids during CT of the sinuses. *Otolaryngol Head Neck Surg.*, 133(4): 531-533.

Bernhardt, T.M., U. Rapp-Bernhardt and A. Fessel, 1998. CT scanning of the paranasal sinuses: axial helical CT with reconstruction in the coronal direction versus coronal helical CT. *Br J Radiol*, 71: 846-851.

Bianchia, S.D., T.O. Rampadob, L. Lubertoa, A.F. Genovesioa, C.C. Bianchia and R. Ropolo, 2005. Image quality analysis and low dose dental CT. *Int Cong Series*, 1281: 1177-1181.

Cardis, E., A. Kesminiene, V. Ivanov, I. Malakhova, Y. Shibata, V. Khrouch and V. Drozdovitch., 2005. Risk of thyroid cancer after exposure to 131I in childhood. *J Natl Cancer Inst.*, 97(10): 724-732.

Cohnen, M., B. Cohnen and K. Ewen, 1998. Dosage measurements in spiral CT examinations of the head and neck region. *Rofo Fortschr Geb Rontgenstr Neuen Bildgeb Verfahr*, 168: 474-479.

Cohnen, M., H. Fischer, J. Hamacher, E. Lins, R. Kötter and U. Mödder, 2000. CT of the head by use of reduced current and kilovoltage: relationship between image quality and dose reduction. *AJNR Am J Neuroradiol*, 21(9): 1654-1660.

Czechowski, J., J. Janeczek and G. Kelly, 2000. Radiation dose to the lens in sequential and spiral CT of the facial bones and sinuses. *Eur Radiol.*, 11: 711-713.

Dammann, F., A. Bode and M. Heuschmidt, 2000. Multislice spiral CT of the paranasal sinuses: first experiences using various parameters of radiation dosage [in German]. *Rofo Fortschr Geb Rontgenstr Neuen Bildgeb Verfahr*, 172: 701-706.

Goldman, L.W., 2007. Principles of CT: Radiation Dose and Image Quality. *J Nucl Med Technol.*, 35: 213-225.

Hojreh, A., C. Czerny and F. Kainberger, 2005. Dose classification scheme for computed tomography of the paranasal sinuses. *Eur J Radiol.*, 56(1): 31-37.

Homolka, P., A. Gahleitner, H. Kudler and R.A. Nowotny, 2001. simple method for estimating effective dose in dental CT Conversion factors and calculation examples for a clinical low dose protocol. *Rofo Fortschr Geb Rontgenstr Neuen Bildgeb Verfahr*, 173: 558-562.

Kearney, S.E., P. Jones and K. Meakin, 1997. CT scanning of the paranasal sinuses—the effect of reducing mAs. *Br J Radiol.*, 70: 1071-1074.

Kim, I.K., J.R. Kim, K.S. Jang, Y.S. Moon and S.W. Park, 2007. Orbital abscess from an odontogenic infection. *Oral Surg Oral Med Oral Pathol Oral Radiol Endod.*, 103: e1-e6.

Lam, S.Y., G. Kumar, K.H. Ng and A.F. Hussain, 2009. A comparison between low-dose and standard-dose noncontrasted multidetector CT scanning of the paranasal sinuses. *Biomed Imaging Interv J.*, 5(3): e13.

Ling, F.T. and S.E. Kountakis, 2006. Advances in imaging of the paranasal sinuses. *Curr Allergy Asthma Rep.*, 6: 502-7.

Loubele, M., R. Bogaerts, E. Van Dijck, R. Pauwels, S. Vanheusden, P. Suetens, G. Marchal, G. Sanderink and R. Jacobs, 2009. Comparison between effective radiation dose of CBCT and MSCT scanners for dentomaxillofacial applications. *Eur J Radiol.*, 71(3): 461-468.

MacLennan, A.C., 1995. Radiation dose to the lens from coronal CT scanning of the sinuses. *Clin Radiol.*, 50: 265-267.

Mettler, Jr, F.A., P.W. Wiest and J.A. Locken, 2000. CT scanning: patterns of use and dose. *J Radiol Prot.*, 20: 353-359.

Mulkens, T.H., C. Broers, S. Fieuws, J.L. Termote and P. Bellnick, 2005. Comparison of Effective Doses for Low-Dose MDCT and Radiographic Examination of Sinuses in Children. *AJR Am J Roentgenol.*, 184: 1611-1618.

Perrella, A., S.S. Rocha and M. Cavalcanti, 2003. Quantitative analysis of maxillary sinus using computed tomography. *J Appl Oral Sci.*, 11(3): 229-233.

Sales, M.A. and M.G. Cavalcanti, 2009. Complex odontoma associated with dentigerous cyst in maxillary sinus: case report and computed tomography features. *Dentomaxillofac Radiol.*, 38: 48-52.

Shrimpton, P.C., D.G. Jones and M.C. Hillier, 1999. Survey of CT practice in the UK, Part 2: Dosimetric aspects. London: HMSO.

Sohaib, S.A., P.D. Peppercorn and J.A. Horrocks, 2001. The effect of decreasing mAs on image quality and patient dose in sinus CT. *Br J Radiol.*, 74: 157-61.

Stelmach, R., S.A. Junior, C.M. Figueiredo, K. Uezumi, A.M. Genu, R.M. Carvalho-Pinto and A. Cukier, 2010. Chronic rhinosinusitis in allergic asthmatic patients: radiography versus low-dose computed tomography evaluation. *J Asthma Aug.*, 47(6): 599-603.

Tack, D., J. Widelec, V. De Maertelaer, J.M. Bailly, C. Delcour and P.A. Gevenois, 2003. Comparison between low-dose and standard-dose multidetector CT in patients with suspected chronic sinusitis. *AJR Am J Roentgenol.*, 181(4): 939-944.

Tan, T.Y., S. Shashinder, V. Subrayan and G. Krishnan, 2008. Silent sinus syndrome due to a maxillary mucocele. *Auris Nasus Larynx*, 35: 285-287.

Yu, L., T.J. Vrieze, M.R. Bruesewitz, J.M. Kofler, D.R. DeLone, J.F. Pallanch, E.P. Lindell and C.H. McCollough, 2010. Dose and Image Quality Evaluation of a Dedicated Cone-Beam CT System for High-Contrast Neurologic Applications. *AJR Am J Roentgenol*, 194(2): W193-W201.

Zammit-Maempel, I., C.L. Chadwick and S.P. Willis, 2003. Radiation dose to the lens of eye and thyroid gland in paranasal sinus multislice CT. *Br J Radiol.*, 76(906): 418-420.

Zammit-Maempel, I., 1996. Radiation dose to the lens of eye and thyroid gland from coronal sinus CT. *Br J Radiol Congress Supplement*, 69: 191.